Maejo Int. J. Sci. Technol. **2010**, *4*(03), 435-445

Maejo International
Journal of Science and Technology

ISSN 1905-7873
Available online at www.mijst.mju.ac.th

Communication

Feature extraction of near-spherical fruit with partial occlusion for robotic harvesting

Lü Qiang [1, 2], Lu Huazhu [1], Cai Jianrong [1,*], Zhao Jiewen [1], Li YongPing [3] and Zhou Fang[1]

[1] School of Food and Biological Engineering, Jiangsu University, Zhenjiang, Jiangsu, 212013, China
[2] School of Information Science and Engineering, Henan University of Technology, Zhengzhou, 450001, China
[3] School of Art Education, Jiangsu University, Zhenjiang, 212013, China

* Correspondence author, e-mail: lvqiang1111@gmail.com

Received: 2 December 2009 / Accepted: 12 October 2010 / Published: 20 October 2010

Abstract: For a fruit-picking robot in natural scenes, feature extraction of fruits occluded by leaves and branches based on machine vision is a key problem. In this study, the cluster barycentre (CB), edge barycentre (EB), circular Hough transform (CHT) and least square circle fitting (LSCF) are used to extract the features of fruit. The results indicate that the first two methods cannot accurately determine the circle in the presence of partial occlusion. The objects extracted by the CHT method include false targets in addition to longer time and larger memory required. The LSCF method, on the other hand, can accurately extract the features in a real-time mode. When the occluded area ratio is less than 52%, or the occlusion angle is less than 216°, the accuracy of feature extraction using LSCF can meet the requirements of the robot operation.

Keywords: near-spherical fruits, machine vision, least square circle fitting (LSCF), feature extraction, robotic harvesting

---

INTRODUCTION

Owing to labour shortage and high labour cost, the cost of manual harvesting accounts for over 40% of the total cost in citrus production [1]. Mechanical mass harvesting is unsuitable for fresh agricultural products for it usually damages the fruits and trees. Robotic selective harvesting is an effective way to cope with labour shortage and rise of production cost, and to meet the need of harvesting fresh agricultural products.

The use of robots to pick tree fruits was proposed by Schertz and Brown in a review of citrus mechanical harvesting system in 1968 [2]. In the past forty years, studies on robotic harvesting of oranges [3-5], apples [6-7], strawberry [8-9], tomatoes [10-12] and other fruits were reported. The increasing computational power and the availability of advanced sensors and robotic technology have facilitated the development of robotic harvesting technology. However, robotic harvesting is not yet commercially available. The challenges for robotic selective harvesting as suggested by Sarig [13] are the vision system for fruit recognition and location, the end-effector for fruit removal and the coordination of these two components.

Fruit recognition and location are the priority of harvesting robot. Machine vision, thermal imaging and laser ranging techniques were used to realise these operations by some researchers [14-15]. Considering the working efficiency, machine vision has become preferred. In general, the machine vision system of a harvesting robot is composed of a binocular camera which acquires images in the scene and a computer programmed to recognise and locate the desired objects through image segmentation, feature extraction, stereo match, and three-dimensional measurement techniques.

A fruit can be segmented from the background in the scene where significant colour contrast exists between the fruit (such as apples, oranges and tomatoes) and the canopy. However, the existence of overlapping of objects and the occlusion by branches and leaves in the unstructured natural scenes make it difficult to segment complete fruit region. All of these result in the deviation in feature extraction and spatial location. An appropriate method which can accurately extract features from incomplete target images has become one of the key research targets of harvesting robot. For positioning of near-spherical fruit, spatial features such as the centre coordinate and radius must be extracted. In a 2D image, the fitting circle of fruit contour can be used to present the object, where the centre and radius of the circle are the features.

The simplest solution to circle fitting is to compute the barycentre of the cluster of object region pixels (cluster barycentre method, CB) [16-18]. In this simple approach, the radius of the circle can be estimated as the maximum distance of the pixels from the barycentre. To reduce the calculation, the edge barycentre method (EB) was proposed, which only considers the boundary pixels, and the radius is computed as the mean distance of the boundary pixels from the estimated centre [16-18]. These approaches, however, do not take full advantage of our knowledge of a circle's shape and more refined parametric approaches have been proposed. The circular Hough transform (CHT) and its modification were used to locate centres of objects based on their contours and do not require the full outline of the objects [19-21]. Using both the edge and the directional images, a modified CHT was applied to detect circular arcs that should correspond to tomato contours [19]. The obtained results were very sensitive to the user-specified threshold value and the best result for a 99% threshold value was 68% correct detection and 42% false detection. The contour of the leaves was one of the major problems since the analysis algorithm interpreted them as possible fruits. Grasso and Recce [22] used CHT to estimate the locations of centres based on the citrus edges in natural scenes. The authors reported problem when oranges were partially occluded by leaves. Cai et al. [21] used modified CHT to extract the centre coordinates and radii and recover the shapes of citrus without occlusion or with slight occlusion.

Although CHT is a simple approach to detect near-spherical fruit, it is a computationally intensive approach with respect to time and memory. The main alternative method for the detection and analysis of near-circular features is the least-square circle fitting (LSCF). Researches in which least-square fitting of circles has been used in astronomy, physics, biology, quality control and metrology can be found reported in the literature [17, 23-26]. The main objectives of this investigation are: 1) to find a suitable method to fit circles and extract features that can represent the near-spherical fruit (citrus, apples, pears, tomatoes, etc.), and 2) to analyse the impact of the extent of occlusion or overlapping on feature extraction.

MATERIALS AND METHODS

Materials

The near-spherical citrus tested in this study was planted in Jiangxinzhou, Zhenjiang City, China. The fruit (commonly called Miyagawa) are primarily sold in the fresh market. Therefore, selective harvesting is the best way to maximise the market value of the fruit. The equatorial or long diameter of the harvested fruit ranges between 60-78 mm. The equatorial diameter and height (short diameter) of the single fruit used for this laboratory analysis were 71.2 mm and 64.6 mm respectively.

Image Acquisition

Citrus images were obtained in a self-made image acquisition device composed of a light box with diffuse illumination, a charge coupled device and a host computer. Diffusers were installed in the light box wall as well as the dome. Multiple internal reflection caused the light to show no preferred direction. There was no shadow or strong reflection in the images. The camera of the charge coupled device was a LU075C (Lumenera Corporation, Canada). The main controlling computer had a Pentium IV CPU (3.0 GHz) and a memory of 1.5 G. All images were digitised into 640×480×24-bit colour bitmap images in RGB (red, green, blue) colour space.

The sample citrus was fixed at the centre of a white bottom, the citrus equator being perpendicular to the floor. A total of 56 images of the citrus were obtained in the laboratory, the first one being that of the unoccluded fruit and the rest, those of the fruit occluded with leaves (Figure 1). The occluded area ranged from 0 to 94% and the occluded contour angle ranged from 0 to 320°. Only one fruit sample was used to capture all the 56 images and during the image acquisition, the citrus fruit was not moved to ensure that its central location was unchanged.

An image for the validation test was captured in October of 2008 in a natural scene of an orchard using the same camera and computer.

Software

In this work, the images were captured and processed by a self-developed software based on Visual C++ 2008 (Microsoft Co., USA), LuCam SDK V4.2 (Lumenera Corporation, Canada) and MVTec Halcon 8.0 (MVTec Software GmbH, Germany) software platforms.

Image Segmentation

Segmentation separates the object (fruit) of interest from the background, which is the first step for object recognition. Its performance is critical to fruit detection since the segmentation output serves

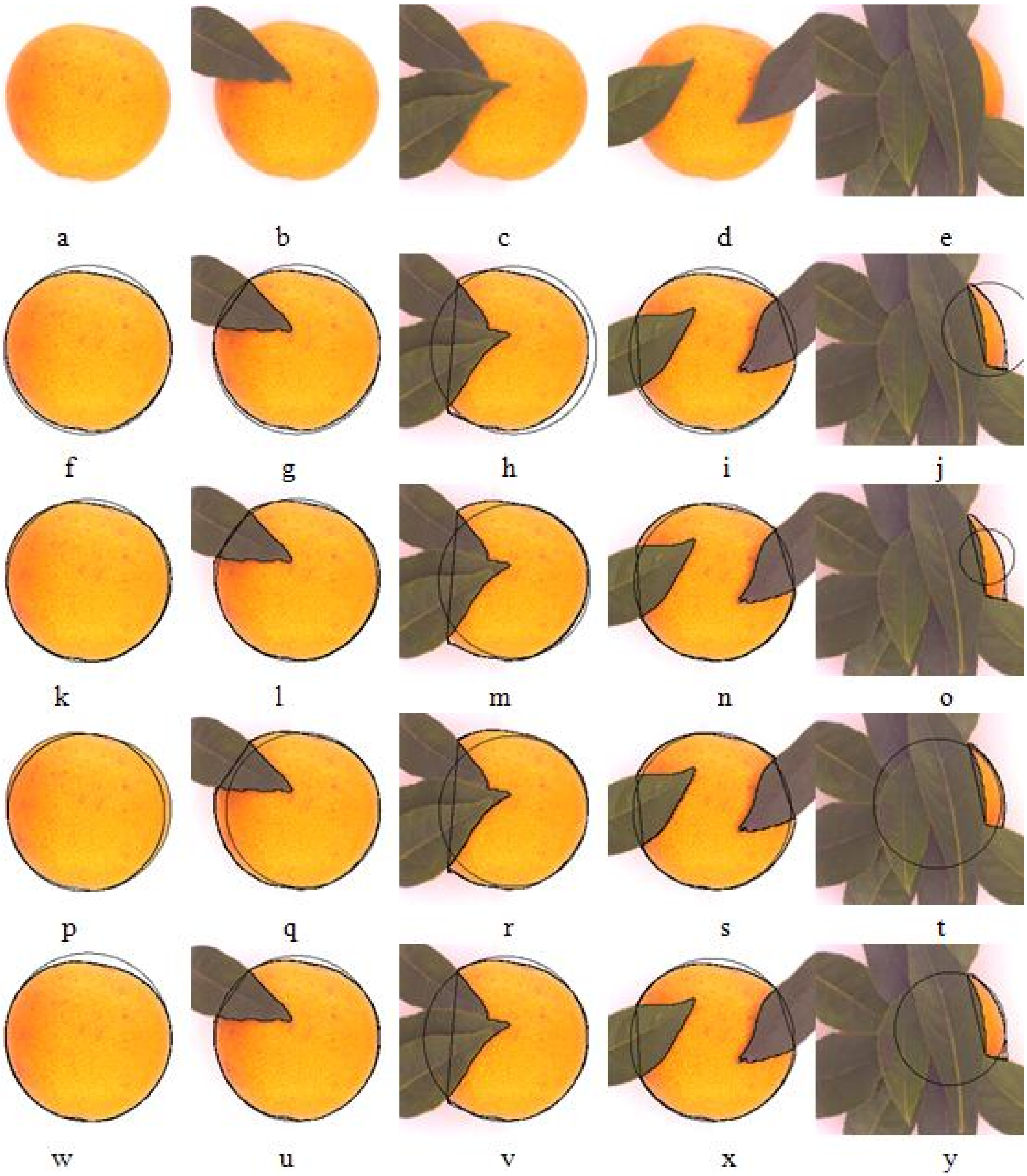

Figure 1. Fitting circles of five images using different methods. In the first row (a-e), the original images are shown. The images shown in 2nd, 3rd, 4th and 5th rows are fitted using CB, EB, CHT and LSCF respectively.

as input to succeeding processes. In occluded citrus images obtained in the lab, object (foreground) segmentation from the background (leaves and white paper) was simple. In this study, all the images were decomposed into R, G and B (red, green and blue) component images at first. By analysing the grey values and grey histograms of the component images and colour difference images, it was found that there was an obvious difference between citrus and background in the G-B colour difference images, and this difference did not exist in other component images. In computer vision, Otsu algorithm [27]was used to automatically perform histogram-shape-based image thresholding. The citrus (foreground) regions were segmented using Otsu method. Then the holes in the fruit region were filled using hole filling.

The next step was the removing of the regions which did not correspond to the physical citrus in the binary image. The regions can have several properties and an important one is the area. This property can remove any region that is too small to be an object. So the regions were removed using size filtering and the citrus binary images were then obtained.

Due to occlusion by leaves and branches, many citrus images were incomplete, and there were different degrees of concave, which had a great impact on the circle fitting. Convex hull operation [28-29] was used to eliminate concaves and reduce their impact for fitting.

Feature Extraction

To locate a near-spherical fruit in a 2-D image, the coordinate of its centre and its radius can be accessed through circle fitting of the fruit region. In this paper, all the four approaches (CB, EB, CHT and LSCF) were used to extract the fruit's features.

In CB method, the fruit centre was the barycentre of the object cluster and the radius could be estimated as the maximum distance of the pixels from the barycentre. So the features could be computed using the citrus binary images. The results of CB are shown in Figure 1(f-j).

The other three approaches for feature extraction needed citrus contours. The contours could be obtained using edge detection. In EB method, only the boundary pixels could be considered. The centre was the barycentre of the boundary and the radius was computed as the mean distance of the border pixels from the estimated centre. The results of EB are shown in Figure 1(k-o).

Circular Hough transformation (CHT)

In image processing, CHT is widely adopted as a circle can be defined by a triplet of values, i.e. $(\mathrm{pc}, R\mathrm{c})$, where $\mathrm{pc} = (x_c, y_c)$ is the circle's centre and $R\mathrm{c}$ is its radius. Then the $(\mathrm{pc}, R\mathrm{c})$ space can be discretised into a finite number of accumulation cells, each corresponding to a specific circle, and a counter is linked with it. In this method, the whole edge pixels are extracted firstly from the image: $\{P_i\}_{i=1\cdots N}$. Then for each P_i, the counters of all those cells $(\mathrm{pc}, R\mathrm{c})$ that are compatible with P_i are increased by one. When all the points have been considered, the most probable circle centre and radius are included in the accumulation cell with the highest count. However, this is not easy to implement, and the CHT method is very slow. Moreover, it needs a large room for memory to reach a relatively high accuracy since accuracy is proportional to the size of the discretised cells [30-31]. The results of CHT are shown in Figure 1(p-t).

Least-square circle fitting (LSCF)

To fit a circle through all points $\{P_i(x_i, y_i)\}_{i=1\ldots N}$ of the contour, an error is defined for each point P_i as the distance between P_i and the circumference. The cost function is defined as:

$$E = \sum_{i=1}^{N} (\rho_i - R_c)^2 \qquad (1)$$

where $\rho_i = \|P_i - P_c\| = \sqrt{(x_i - x_c)^2 + (y_i - y_c)^2} \qquad (2)$

is the distance of a generic point from the circle's centre. P_c is the centre of the fitting circle and R_c is its radius. The cost function minimisation leads to a non-linear optimisation which can be solved iteratively using non-linear optimisation techniques [32].

The LSCF is not robust to large outliers since points that lie far from the circle have a very large weight in the optimisation because of the squared distance. To reduce the influence of distant points, we can introduce a weight function for the points. The Huber weight function and Tukey weight function are usually used [32]. In this study, we used Tukey weight function, which is given by:

$$\omega(\delta_i)=\begin{cases}[1-(\delta_i/\tau)^2]^2 & (|\delta_i|\le\tau)\\ 0 & (|\delta_i|>\tau)\end{cases} \tag{3}$$

where τ is the clipping factor and δ_i is the distance of the points to the circle. The cost function becomes:

$$E=\sum_{i=1}^{N}\omega_i(\rho_i-R_c)^2 \tag{4}$$

The object circle can be gained through minimising iterations of the functions. The results of LSCF are shown in Figure 1(w-y).

Measurement of Occlusion

Different kinds and degrees of occlusion partially hiding the citrus fruit can lead to the reducing of visible area and incomplete extraction of the original contour of the citrus. As the occlusion degrees vary, the feature extraction accuracy also does. For each image obtained in the lab, the occluded area ratio (R_{oa}) and the occluded angle (θ_o) were defined to represent the occlusion level of the object. R_{oa} was defined as:

$$R_{oa}=(1-\frac{Area_v}{Area_u})\times 100\% \tag{5}$$

where $Area_u$ is the area of the unoccluded citrus computable from the first image, and $Area_v$ is the visible area of the citrus with various degrees of occlusion. Occluded contours may have only one paragraph or more paragraphs (Figure 1d and Figure 2). θ_o is defined as the sum of every occluded angle (Figure 2), which can be computed by the following formula:

$$\theta_o=\sum_{1}^{N}\theta_i \tag{6}$$

where N is the number of occluded paragraphs of fruit contour, θ_i is the angle of occluded paragraph No. i, which can be obtained through the law of cosines. By calculation, R_{oa} ranged from 0 to 94%, and θ_o ranged from 0 to 320° in this experiment.

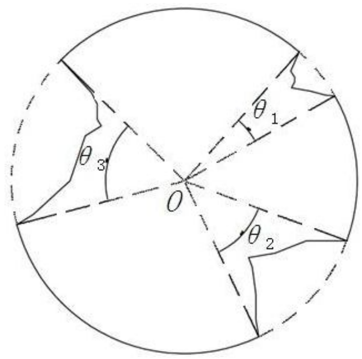

Figure 2. Diagram of occluded angles of fruit

RESULTS AND DISCUSSION

Analysis for Simulation Examples

The proposed algorithms were tested by the images obtained both in the laboratory and in the field, and the relationship between feature extraction accuracy and occlusion was analysed. For all methods, the higher the occlusion level was, the stronger the impact on the feature extraction became (Figure 1). The following indicators, viz. radius ratio (r_r) and ratio of centre offset (r_c), were used to evaluate the feature extraction accuracy. They were defined as:

$$r_r = \frac{r_o}{r_u} \tag{7}$$

where r_u is the radius of fruit without occlusion and r_o is the radius of fruit with occlusion; and

$$r_c = \frac{D}{r_u} \tag{8}$$

where D is the distance between the centres of the citrus with and without occlusion. From Figure 1(f, k, p and w), it could be found that r_u and the centres were different with different methods.

The performance of the feature extraction using CB, EB, CHT and LSCF was compared quantitatively and the results are shown in Figures 1 and 3. To position accurately the objects on the tree, the criteria of the feature extraction were set so that the radius ratio (r_r) was not less than 90% and the ratio of centre offset (r_c) was not more than 10%. Results of the feature extraction using different algorithms under different occluded area ratios and angles are shown in Figure 3. In order to meet the demand of the feature extraction, the thresholds of R_{oa} and θ_o for different methods, shown in Table 1, were applied.

From Figure 3 and Table 1, it was found that the impacts of occlusion on the feature extraction for CB and EB were greater than those for CHT and LSCF. To meet the criteria of the feature extraction, the occluded area ratios (R_{oa}) when using CB, EB, CHT and LSCF algorithm, were to be less than 25%, 27%, 54% and 52% respectively, or the occlusion angles (θ_o) less than 95°, 100°, 222° and 216° respectively.

With the increase of occlusion degree, the error of the feature extracted rose. The impact of contour occlusion on the feature extraction was greater than that of area occlusion. The curvature stability and continuity of the remaining contour had a great influence on the feature extraction. If the contour curvature remained relatively stable, when occlusion angle reached up to 268°, the centres and radii were better extracted using CHT or LSCF. When the visible areas were equal in different occlusion, the longer the remaining contour was, the higher the extraction accuracy became.

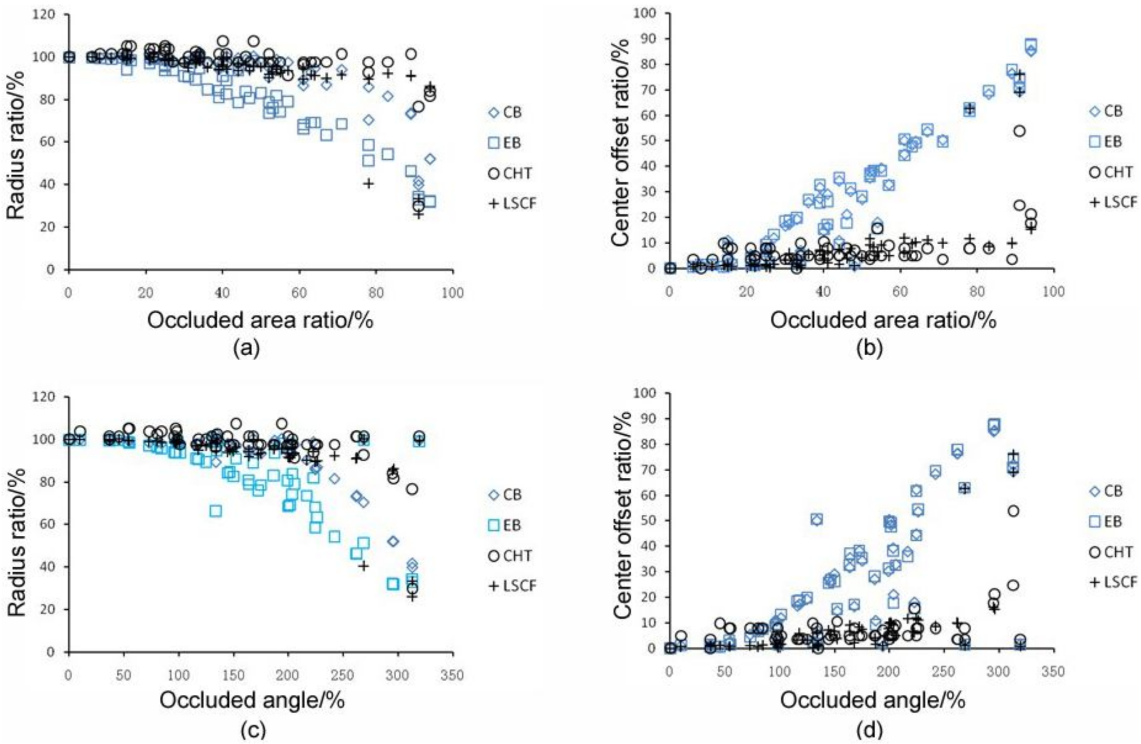

Figure 3. Distribution of feature extraction measurement: (a) radius ratio vs. occluded area ratio; (b) centre offset ratio vs. occluded area ratio; (c) radius ratio vs. occluded angle; (d) centre offset ratio vs. occluded angle

Table 1. Thresholds to meet the requirements of feature extraction using different methods

	$r_r \geq 90\%$		$r_c \leq 10\%$		$r_r \geq 90\%$ & $r_c \leq 10\%$	
	R_{oa} (%)	θ_o (°)	R_{oa} (%)	θ_o (°)	R_{oa} (%)	θ_o (°)
CB	<60	<224	<25	<95	<25	<95
EB	<33	<124	<27	<100	<27	<100
CHT	<90	<290	<54	<222	<54	<222
LSCF	<70	<268	<52	<216	<52	<216

Due to occlusion, the precision of extraction inevitably declined for lack of the original contour. In this study, convex hull operation was used to reduce the impact of occlusion concaves by repairing the occlusion to a certain extent.

The CB and EB apparently could not effectively extract the features. The reasons were the poor performance by using the barycentre of the cluster or edge as the fruit centre and by calculating the maximum or mean distance of the boundary pixels from the centre as the radius. The CHT and LSCF, on the other hand, worked well and could be used to extract the features of near-spherical fruit.

However, the accuracy of the CHT was limited when the accumulation cells discretised. Decreasing the size of the accumulation cells drastically increased computation time, making the CHT practically useless for many applications, especially ones that required real-time processing.

Analysis in Natural Scenes

In a natural scene, images of multiple objects are captured by the fruit-picking robot. The features of the fruit with different sizes require a suitable algorithm for real-time extraction. There are 22 fruits in the image shown in Figure 4(a); 18 of them were segmented using Otsu algorithm on G-B, size filtering, hole filling, watershed segmentation employing distance transform, convex hull operation and roundness filtering.

The features of all the 18 fruits could be extracted using LSCF as shown in Figure 4(b). By CHT, 18 objects were gained including 2 false objects and 2 fruit had not been extracted (Figure 4(c)). In the feature extraction of these 18 objects in this image, LSCF required 44.60 ms while CHT required 92.91 ms (more than twice as long as for LSCF). Moreover, comparing Figures 4(b) and 4(c), the features obtained by LSCF were more accurate in presenting objects than those obtained by CHT.

(a) (b) (c)

Figure 4. Feature extraction of images obtained in a natural scene: (a) original image; (b) feature extraction using LSCF; (c) feature extraction using CHT

CONCLUSIONS

The CB, EB, CHT and LSCF methods were presented and used to extract the features of near-spherical fruit in 2-D images. It was also shown with simulation and real examples that the LSCF could locate the centre and estimate the radius of the fruit accurately, reliably and in a real-time mode, even in the presence of partial occlusion. If the occlusion area ratio was less than 52% or the occlusion angle was less than 216°, the object could be located accurately, suggesting that this algorithm can be used for designing the fruit-picking robot in natural scenes.

ACKNOWLEDGEMENTS

This work has been financially supported by the National High Technology Research and Development Program of China (Project No. 2006AA10Z263) and the National Natural Science Foundation of China (Project No. 30771243).

REFERENCES

1. G. K. Brown, "Mechanical harvesting system for the Florida citrus juice industry", ASAE Paper No. 021108, ASAE Annual International Meeting, **2002,** St. Joseph, Michigan, USA.
2. C. E. Schertz and G. K. Brown, "Basic considerations in mechanizing citrus harvest", *Trans. ASAE*, **1968**, *11*, 343-346.
3. R. C. Harrell, P. D. Adist, T. A. Pool and R. Hoffman, "The Florida robotic grove-lab", *Trans. ASAE*, **1990**, *33*, 391-399.
4. G. Rabatel, A. Bourely, F. Sevila and F. Juste, "Robotic harvesting of citrus: State-of-art and development of the French Spanish Eureka project", Proceedings of the International Conference on Harvest and Post-harvest Technologies for Fresh Fruits and Vegetables, **1995**, Michigan, USA, pp. 232-239.
5. M. Hannan, T. F. Burks and D. M. Bulanon, "A real-time machine vision algorithm for robotic citrus harvesting", ASABE Paper No. 073125, ASABE Annual International Meeting, **2007,** Minneapolis, Minnesota, USA.
6. A. G. D'Esnon, G. Rabatel and R. Pellenc, "A self-propelled robot to pick apples", ASAE Paper No.87-1037, ASAE Annual International Meeting, **1987,** St. Joseph, Michigan, USA.
7. Z. X. Liu and G. Liu, "Apple maturity discrimination and positioning system in an apple harvesting robot", *New Zealand J. Agr. Res.*, **2007**, *50*, 1103-1113.
8. S. Arima, N. Kondo and M. Monta, "Strawberry harvesting robot on table-top culture", ASAE/CSAE Paper No.043089, ASAE/CSAE Annual International Meeting, **2004**, Ottawa, Canada.
9. T. Shiigi, N. Kondo, M. Kurita, K. Ninomiya, J. Kamata, S. Hayashi, K. Kobayashi, K. Shigematsu and Y. Kohno, "Strawberry harvesting robot for fruits grown on table top culture", ASABE Paper No.084046, ASABE Annual International Meeting, **2008**, Providence, Rhode Island, USA.
10. M. Monta, N. Kondo and K. C. Ting, "End-effectors for tomato harvesting robot", *Artif. Intell. Rev.*, **1998**, *12*, 11-25.
11. P. Ling, R. Ehsani, K. C. Ting, N. Ramalingam, M. H. Klingman, Y. Chi and C. Draper, "Sensing and end-effector for a robotic tomato harvester", ASAE/CSAE Paper No.043088, ASAE/CSAE Annual International Meeting, **2004**, Ottawa, Canada.
12. N. Kondo and K. C. Ting, "Robotic for bioproduction systems", America Society of Agricultural Engineering Publisher, Michigan, **1998**, pp.195-212.
13. Y. Sarig, "Robotics of fruit harvesting: A state-of-the-art review", *J. Agr. Eng. Res.*, **1993**, *54*, 265-280.
14. A. R. Jiménez, A. K. Jain, R. Ceres and J. L. Pons, "Automatic fruit recognition: a survey and new results using range/attenuation images", *Patt. Recog.*, **1999**, *32*, 1719-1736.
15. A. R. Jiménez, R. Ceres and J. L. Pons, "A vision system based on a laser range-finder applied to robotic fruit harvesting", *Mach. Vision Appl.*, **2000**, *11*, 321-329.
16. M. S. Shafiq, S. T. Tümer and H. C. Güler, "Marker detection and trajectory generation algorithms for a multicamera based gait analysis system", *Mechatronics*, **2001**, *11*, 409-437.
17. M. Berman. "Large sample bias in least squares estimators of a circular arc centre and its radius", *Comput. Graph. Image Process.*, **1989**, *45*, 126-128.

18. I. Frosio and N. A. Borghese, "Real-time accurate circle fitting with occlusions", *Patt. Recog.*, **2008**, *41*, 1041-1055.
19. A. D. Whittaker, G. E. Miles, O. R. Mitchell and L. D. Gaultney, "Fruit location in a partially occluded image", *Trans. ASAE*, **1987**, *30*, 591-596.
20. J. Illingworth and J. Kittler, "A survey of the Hough transform", *Comput. Vision Graph. Image Process.*, **1988**, *44*, 87-116.
21. J. R. Cai, X. J. Zhou, Y. L. Li and J. Fan, "Recognition of mature oranges in natural scene based on machine vision", *Trans. Chinese Soc. Agri. Eng.*, **2008**, *24*, 175-178 (in Chinese).
22. G. M. Grasso and M. Recce, "Scene analysis for an orange picking robot", Proceedings of the 6th International Congress for Computer Technology in Agriculture, **1996**, Wageningen, The Netherlands, pp. 275-280.
23. S. J. Ahn, W. Rauh and H. J. Warnecke, "Least-squares orthogonal distances fitting of circle, sphere, ellipse, hyperbola, and parabola", *Patt. Recog.*, **2001**, *34*, 2283-2303.
24. L. Moura and R. Kitney, "A direct method for least-squares circle fitting", *Comput. Physics Commun.*, **1991**, *64*, 57-63.
25. W. Gander, G. H. Golub and R. Strebel, "Least-squares fitting of circles and ellipses", *BIT Numer. Math.*, **1994**, *34*, 558-578.
26. N. Chernov and C. Lesort, "Least squares fitting of circles", *J. Math. Imag. Vision*, **2005**, *23*, 239-252.
27. N. Otsu, "A threshold selection method from gray-level histograms", *IEEE Trans. Syst. Man Cybern.*, **1979**, *9*, 62-66.
28. I. Barany, T. van Roy and L. Wolsey. "Uncapacitated lot-sizing: The convex hull of solutions", *Math. Program. Studies*, **1984**, *22*, 32-43.
29. A. Melkman. "On-line construction of the convex hull of simple polygon", *Inform. Process. Lett.*, **1987**, *25*, 11-12.
30. P. V. C. Hough, "Method and means for recognizing complex patterns", *US Patent, 3069654* (**1962)**.
31. I. Frosio and N. A. Borghese, "Real-time accurate circle fitting with occlusions", *Patt. Recog.*, **2008**, *41*, 1041-1055.
32. C. Steger, M. Ulrich and C. Wiedemann, "Machine Vision Algorithms and Applications", Tsinghua University Press, Beijing, **2008**, pp.238-247.